DYNAMICS OF INTENSE INHOMOGENEOUS CHARGED PARTICLE BEAMS*

E.G. Souza, A. Endler, R. Pakter†, F.B. Rizzato
Instituto de Física, Universidade Federal do Rio Grande do Sul, Brazil
R.P. Nunes, Instituto de Física e Matemática, UFPel, Universidade Federal de Pelotas, Brazil

Abstract

Inhomogeneous cold beams undergo wave breaking as they move along the axis of a magnetic focusing system; the largest the inhomogeneity, the soonest the breaking. The present analysis however reveals that the wave breaking time is very susceptible to beam mismatch. It is shown that judiciously chosen mismatches can largely extend beam lifetimes. The work includes some recently discussed issues: the presences of fast and slow regimes of wave breaking, and the role of thermal velocity distributions in space-charge dominated beams. In all instances, the theory is shown to be accurate against simulations.

INTRODUCTION

It is well known that magnetically focused beams of charged particles can relax from non-stationary into stationary flows with the associated particle evaporation [1]. This is the case for homogeneous beams with initially mismatched envelopes flowing along the magnetic symmetry axis of the focusing system. Gluckstern [2] showed that initial oscillations of mismatched beams induce formation of large scale resonant islands [3] beyond the beam border: beam particles are captured by the resonant islands resulting in emittance growth and relaxation. A closely related question concerns the mechanism of beam relaxation and the associated emittance growth when the beam is not homogeneous. On general grounds of energy conservation one again concludes that beam relaxation takes place as the coherent fluctuations of beam inhomogeneities are converted into microscopic kinetic and field energies [4]. Recent works actually show that in the case of cold beams relaxation proceeds in two basic steps. Firstly, wave breaking itself pushes particles off the beam. Secondly, ejected particles are heated up as they absorb energy from macroscopic coherent oscillations of the remaining beam core. Wave breaking is therefore the key feature in the relaxation of cold inhomogeneous beams since it produces those particles that will later form the relaxing beam halo.

Two instances leading to wave breaking in inhomogeneous beams have been identified. Originally, a threshold was obtained in terms of gradients in the amplitude of waves propagating across the beam [5, 6]. While below the threshold breaking is absent, above the threshold it is fast. As particles largely displaced from their equilibrium positions are released, they overtake each other in less than one plasma wave cycle. Density singularities and wave breaking are thus created, and particles are pushed off the beam. A more thorough analysis however shows that not only amplitude gradients, but also the formerly neglected gradients of the spatially varying frequency of the density waves is a key factor determining wave breaking [7, 8]. The physical process is different from the previous, as one shows that no threshold exists in this latter case. Particles slowly move out of phase due to small differences in their oscillatory frequencies, until a time when one eventually overtakes another. At that instant the infinite density peak is again formed generating the breaking.

In all the previous discussion, no particular attention is directed toward beam size; the basic interest was the role of beam non uniformity on wave breaking. One should note, however, that since wave breaking is essentially dictated by compressions and rarefactions of beam densities, it may be quite possible that expansions or contractions of the beam transversal size has a noticeable effect on the process. In particular we will show that, contrarily to the homogeneous beam case where envelope mismatch is an undesirable feature, for inhomogeneous beams it may largely delay wave breaking, extending beam lifetime. Analytical treatment can be made if one considers crystalline cold beams which have been attracting a growing amount of interest lately [9]. We shall therefore expose our case with aid of this type of system, introducing moderate temperatures later to study warmer, but space-charge dominated beams.

BEAM PROFILE AND WAVE BREAKING

Consider an axially symmetric, collisionless, unbunched beam moving with constant velocity along z. Ignoring longitudinal smoother gradients, one obtains the relevant fields with help of Gauss's law as one considers the larger transversal gradients. The equation for the radial motion of any cylindrical layer of the beam thus takes the form [8]

$$r'' = -\kappa\, r + \frac{Q(r)}{r}, \qquad (1)$$

primes indicating derivatives with respect to z for stationary beams. $Q(r)$ is a measure of the total charge up to the present radial layer position. It reads $Q(r) = KN(r)/N_t$, where $K = N_t q^2/\gamma^3 m\beta^2 c^2$ is the beam perveance, with $N(r)$ denotintg the number of particles up to radial coordinate r, and N_t their total number. q and m denote the beam

* Work supported by CNPq and FAPERGS, Brazil, and by AFOSR, USA, grant FA9550-09-1-0283.
† pakter@if.ufrgs.br

particle charge and mass, respectively. $\gamma = (1-\beta^2)^{-1/2}$ is the relativistic factor where $\beta = v_z/c$, v_z is the constant axial beam velocity, and c is the speed of light. $\kappa \equiv (qB/2\gamma m\beta c^2)^2$ where B is the constant axial focusing magnetic field.

We suppose that the beam starts off from rest as a cold fluid. Then, while particles do not overtake each other, $Q(r,z)$ may be evaluated for any layer located at radial position r as the initial value $Q(r_0)$, where $r(z=0) \equiv r_0$. In a likewise fashion, one can compute the amount of charge contained between two neighbor layers located at r and $r+dr$ in the form

$$dQ = 2\pi r\rho(r,z)dr = 2\pi r_0\rho(r_0,0)dr_0, \qquad (2)$$

where ρ denotes the particle density of the system. The expression for dQ tells us that the density evolves as

$$\rho(r,z) = \rho(r_0,0)\left(\frac{r_0}{r}\right)\left(\frac{\partial r}{\partial r_0}\right)^{-1}. \qquad (3)$$

Beams with perfectly matched envelopes are the ones for which the initially farthest radial layer r_{b0} is in equilibrium: $r_{b0}^2 = K/\kappa$ from Eq. (1). Eq. (3) reveals that the density function develops a singularity when the orbital equation $r = r(r_0,z)$ becomes multivalued with $\partial r/\partial r_0 = 0$. This point corresponds to a potential barrier not all particles can move across. Some particles do move through the barrier, but some are reflected relaxing the beam via kinetic effects associated with emittance growth. So, it all depends on the behavior of the compressibility factor $\partial r/\partial r_0$ as a function of "time" z. An approximate solution for small oscillations can be obtained from Eq. (1) in the fluid state where $Q(r)$ can be replaced with $Q(r_0)$ as explained earlier:

$$r(z) \approx r_{eq} + A\,\cos(\omega z). \qquad (4)$$

The solution describes an oscillatory motion of amplitude $A \equiv r_0 - r_{eq}$ around an equilibrium point r_{eq} promptly recognized as $r_{eq} = \sqrt{Q(r_0)/\kappa}$ from Eq. (1). The amplitude depends on r_0, and the nonlinearly corrected frequency also does: canonical perturbative theories show that [8, 10]

$$\omega(r_0) = \sqrt{2\,\kappa} + \frac{\sqrt{\kappa}}{6\sqrt{2}}\left(\frac{A}{r_{eq}}\right)^2. \qquad (5)$$

Therefore, if from Eq. (4) one writes down the compressibility factor one arrives at

$$\frac{\partial r}{\partial r_0} = \frac{\partial r_{eq}}{\partial r_0} + \frac{\partial A}{\partial r_0}\cos(\omega z) - z\frac{\partial \omega}{\partial r_0}A\sin(\omega z). \qquad (6)$$

If the amplitude inhomogeneity is sufficiently large that $\partial A/\partial r_0 > \partial r_{eq}/\partial r_0$, wave breaking takes place within a cycle of oscillation as the cosine's phase slips from zero towards π. In this case the last term on the right hand side of Eq. (4) can be safely neglected as a small $\mathcal{O}(A^2/r_{eq}^2)$ quantity. The threshold condition for fast wave breaking dominated by the amplitude gradient can also be written in the convenient form

$$\sqrt{Q} > \frac{\partial Q}{\partial r_0}. \qquad (7)$$

In typical configurations of beams with humped cores and dilute populations near the border, $\partial Q/\partial r_0 \to 0$ and the condition for wave breaking is easily satisfied there. This is the fast regime analyzed in Refs. [5, 6], as mentioned earlier. In addition to this fast regime, another clear fast regime is found as one considers hollow beams, where densities are extremely high near the beam border, and small at the center. In this case, in contrast with the previous, $\partial Q/\partial r_0$ is large near the border and the threshold condition is unlikely to be fulfilled there. On the other hand, near the beam center where $Q \sim \rho r^2$ for a local density ρ, the condition is automatically satisfied for vanishing small densities. In general, beams may display fast wave breaking wherever the density is so small that the charge accretion satisfies $\partial Q/\partial r_0 \to 0$.

When the threshold for the fast wave breaking is not attained, a simple oscillatory process cannot bring the compressibility factor to the state $\partial r/\partial r_0 = 0$. This is where the last term of Eq. (6) begins to play its crucial role. Corrections to the frequency are small, as mentioned, but the respective term present in Eq. (6) grows linearly with the time z. Thus, no matter how small is the inhomogeneity, for sufficiently long periods of time the term involving the frequency derivative will become large enough that $\partial r_{eq}/\partial r_0 \sim z^*\,A\,\partial\omega/\partial r_0$ for a given $z^* = z^*(r_0)$. Neglecting the nonsecular term, at this point the wave breaking singularity $\partial r/\partial r_0 = 0$ will be reached again. The earliest breaking time is the one of physical relevance. It is obtained here as the minimum of $z^*(r_0)$ over all r_0's in the form $z_{wb} \equiv \min_{r_0}\{z^*(r_0)\}$, from which convenient approximations shall be discussed later.

Therefore: (i) Starting from humped core beams with very low densities at the borders, wave breaking is fast and occurs at the beam border. This is the case studied in previous papers where the frequency term was neglected. (ii) Next, as one diminishes the density contrast between beam core and beam border, one enters a slow regime where the rapidly oscillating compressibility factor modulates linearly with z, reaching the wave breaking state $\partial r/\partial r_0 = 0$ after long time periods. This is the case investigated in Ref. [8] where the amplitude term was in turn neglected. We note that in contrast to the fast regime, the slow regime of wave breaking does not involve any threshold. As long as beam inhomogeneities are present, the beam is bound to undergo wave breaking. (iii) Finally, with further increase of the density contrast, now with higher densities near the border, a new zone of fast wave breaking is reached where breaking occurs near the beam center.

CONTROLLING WAVE BREAKING

We now add the effect of a mismatched beam border to an inhomogeneous profile [11]. As argued before, we

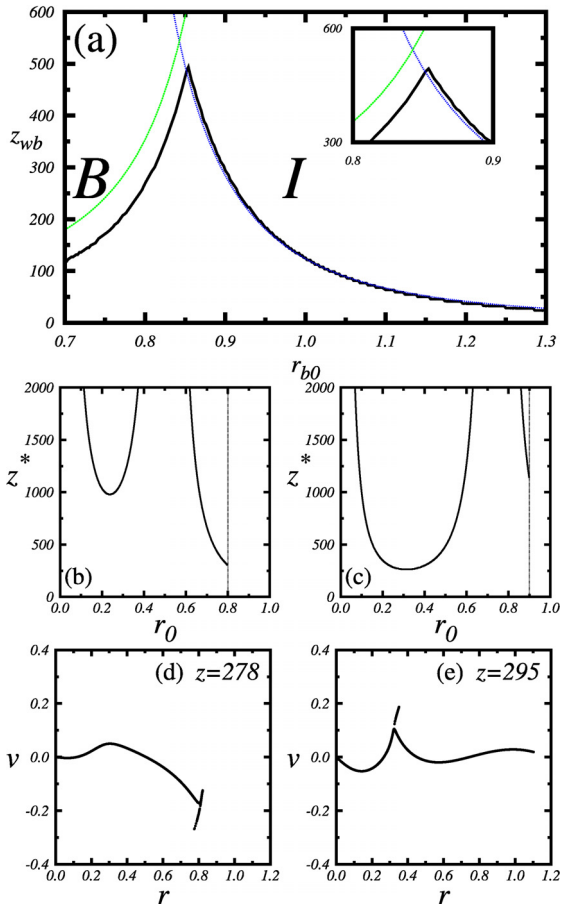

Figure 1: Wave breaking time versus initial beam radius in panel (a). $z^* = z^*(r_0)$ for $r_{b0} = 0.8$ in panel (b) and for $r_{b0} = 0.9$ in panel (c). Beam phase-spaces just after the breaking: $r_{b0} = 0.8$ in panel (d) and $r_{b0} = 0.9$ in panel (e). In all cases, $\chi = 0.6$. All radiuses given in units of $\sqrt{K/\kappa}$ and z in units of $\kappa^{-1/2}$; $v \equiv r'$. Simulations based on Gauss's law using 50000 cylindrical shells.

expect that a beam with varying size may have a significant influence on its inner density distribution and, consequently, on the compressibility factor. We shall investigate the effect in slow regimes, since within the fast regimes a rescaling of beam size has no significant effect on the breaking time. We now need to specify the beam profile we will be working with. It is taken in the general parabolic form

$$\rho(r_0) = \frac{2K}{\pi r_{b0}^2}\left[1 + \chi\left(\frac{2r_0^2}{r_{b0}^2} - 1\right)\right], \qquad (8)$$

for $r_0 \leq r_{b0}$ where r_{b0} is the initial beam size and $-1 \leq \chi \leq +1$ measures the degree of inhomogeneity; $\chi \to -1$ for humped and $\chi \to +1$ for hollow beams. We evaluate the charge as $Q(r_0) = \int_0^{r_0} 2\pi r\rho(r)dr$ and use the result to see that the slow region lies within the borders $\chi_{min} = -0.5$ and $\chi_{max} = 0.75$ for the matched beam $r_{b0} = \sqrt{K/\kappa}$. With that information, to be corroborated later, we construct Fig. 1(a) using $\chi = 0.6$, where the earliest wave breaking time z_{wb} is displayed as a function of beam size. In all forthcoming numerical discussions radial coordinates will be given in units of $\sqrt{K/\kappa}$ and z in units of $\kappa^{-1/2}$. Note that because of our choice of the inhomogeneity $\chi = 0.6$, we do fall in a slow region, at least in the vicinity of the matched beam. The thick line is obtained exactly as one integrates Eq. (1) and its derivative with respect to r_0, all in the fluid state where we can replace $Q(r) \to Q(r_0)$. The thin lines, whose origins will be discussed shortly, are based on the perturbative solution Eq. (6) and approximate the exact curve on the right and left sides of the peak. In addition to the peak the plot reveals strong sensitivity to the choice of r_{b0}. We note that the matched beam is not the one with the largest lifetime before breaking. The longest living beam is the one at the peak where $r_{b0} \approx 0.85$, and its breaking time is around five times larger than the matched beam's time. The reason for the sharp peak can be understood in panels (b) and (c) where we plot the local wave breaking time $z^*(r_0)$ as a function of the initial position of the corresponding fluid element; as mentioned earlier, the earliest (smallest) breaking time is the one of physical significance. Panel (b) represents one point $r_{b0} = 0.8$ on the left side of the peak. For this point and all others on the left side the earliest breaking occurs at the beam border (B). Panel (c) represents the point $r_{b0} = 0.9$ on the right side of the peak of panel (a), and reveals that the earliest breaking time for this point (and all others on the right side) occurs in the inner (I) body of the beam. The curves for $r_{b0} < 1$ always reveal two local minima separated by a divergent z^*. The divergent point corresponds to a fixed equilibrium point located inside the beam; that portion of the beam extending up to the fixed point behaves like a matched beam of smaller radius than the whole. This helps to obtain the wave breaking time z_{wb}^I in the inner region (rhs approximation) as one can use minimizing procedures applied to fully matched beams [8]:

$$z_{wb}^I = \left(\frac{3}{2\kappa}\right)^{1/2} \frac{\alpha^3\left(4\sqrt{1-\chi'} + \chi' - 1\right)}{\left(\sqrt{3} - \alpha\right)^2\left(\sqrt{1-\chi'} + \chi' - 1\right)}, \qquad (9)$$

where $\alpha \equiv (1 + 2\sqrt{1-\chi'} - \chi')^{1/2}$ and $\chi' = 1 + (\chi - 1)K/\kappa r_{b0}^2$ is a renormalized inhomogeneity factor. As for the wave breaking time at the beam border z_{wb}^B (lhs approximation) one simply evaluates $z_{wb}^B = z^*(r_0 = r_{b0})$:

$$z_{wb}^B = 3\sqrt{2}(\chi+1)\left[r_{b0}\sqrt{\kappa/K}(r_{b0}\sqrt{\kappa/K} - 1)^2\chi\right]^{-1}. \qquad (10)$$

There is thus an abrupt transition between these two regimes precisely at the peak, where the beam simultaneously breaks at the center and at the border: r_{b0} at the peak is obtained from $z_{wb}^I = z_{wb}^B$. We also perform full N-particle simulations based on Gauss's law [12] using 50000 cylindrical shells. The simulation results shown in panels (d) ($r_{b0} = 0.8$) and (e) ($r_{b0} = 0.9$) of Fig. 1, confirm the abrupt transition. When $\chi < 0$ the behavior is reversed, but

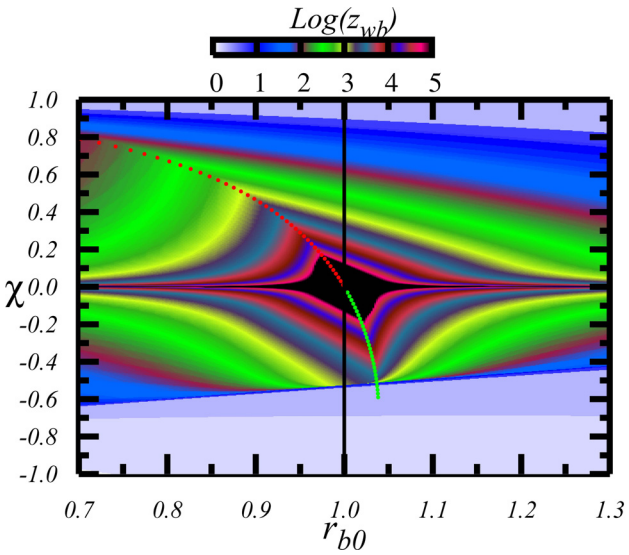

Figure 2: Wave breaking time map in the $\chi \times r_{b0}$-space. Colors are related with magnitude of the wave breaking time. Doted line comes from the analytical approach, and indicate the loci of maximum wave breaking time. Black means $z_{wb} > 10^5$.

otherwise equivalent, with the internal fixed point appearing when the beam is stretched with $r_{b0} > 1$.

We now investigate the roles of size and profile in a unified way. To do so we construct Fig. 2 where the earliest breaking time is coded in colors, as a function of the control parameters r_{b0} and χ. The plot covers a wide range along the horizontal axis and covers the full χ range $-1 < \chi < 1$, enabling the see the fast wave breaking regions and all details of the slow region. The bent dotted line represents the loci of the largest wave breaking time. What was suggested in Fig. 1 is fully confirmed here: wave breaking strongly depends not only on the beam profile χ, but also on the beam size r_{b0}; see expression for χ'. And more: Fig. 1(a) teaches how a judicious mismatching applied to r_{b0} may help to control the deleterious effects of non uniformities across the beam section. Even the borders of the fast regions respond to the mismatch: if for a given χ one is not too deep into the fast regions, a shift in r_{b0} can bring the system into the slower region of wave breaking. Note that previous estimates for the matched beam zoning are accurate.

THERMAL BEAMS

The relevance of crystalline beams has been reported in a series of recent works [9, 8], but one might wonder how the theory applies to space-charge dominated, but warmer beams [13]. Is it still possible to control the extent of the fluid-like state prior to relaxation with help of convenient mismatches applied to the beam envelope size? To answer the question the reader is referred to Fig. 3 where we ana-

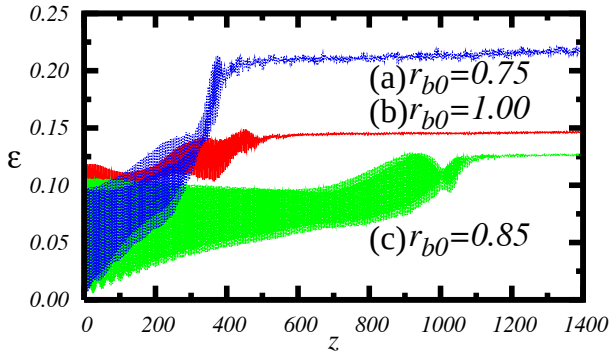

Figure 3: Relaxing emittance for various r_{b0}'s, all cases with a small initial velocity spread $\Delta v = 1.6\times10^{-2}$ around $v = 0$; velocity in units of $\sqrt{K}$.

lyze the issue. In all cases we start with particles spatially distributed according to the parabolic $\rho(r_0, \chi)$, but with a small and uniform normalized velocity spread of width $\Delta v = 0.016$ around the axis $v = 0$. Emittance growth is used as a tool to measure thermal effects and beam relaxation. Emittance ε is evaluated as the average, $<>$, over all beam particles: $\varepsilon = 2\sqrt{< r^2 >< v^2 > - < rv >^2}$.

Particles are ejected from the cold core providing a numerous population that can be accelerated by the remaining oscillating core to create a diffuse halo. As the halo is established, coherent beam oscillations relax and beam emittance saturates. Emittance initially oscillates while the beam behaves mostly as a regular fluid; emittance compensating techniques can be applied here to reduce the effects of oscillations on beam quality [14]. Relaxation is attained later when the emittance evolves to the flat line, thermal regime of the figure. r_{b0} for curves (a) and (c) are symmetrically located around the peak $r_{b0} \approx 0.85$ of Fig. 1(a), both corresponding to the same z_{wb}. Fig. 3 reveals that their relaxation times are similar and smaller than curve (b) where we represent the point associated with the peak $r_{b0} \approx 0.85$. The trend associated with the role of mismatch thus remains the same as observed in the cold wave breaking calculations: one can considerably postpone the thermal regime with an adequate choice of the initial beam size.

CONCLUSION

To conclude, we find two types of wave breaking situations in space charge inhomogeneous beams: a fast breaking commanded by amplitude gradients of density waves across the beam, and in its absence, a slow breaking commanded by frequency gradients. The latter has no threshold and is bound to happen no matter how small is the beam non uniformity. Then, in all instances, we showed how a judiciously chosen envelope size mismatch can significantly extend the beam life time as compared with the traditional perfectly matched case. Finally, small thermal

effects were considered, to show that even warmer beams can still be well controlled with envelope mismatches. The present investigation is concerned with control of irreversible growth of thermal emittance in beams displaying non laminar transverse motion. Our results show that convenient envelope mismatches provide a desirable degree of control.

REFERENCES

[1] M. Reiser *Theory and design of charged particle beams*, John Wiley, New York, (1994); A. Cuchetti, M. Reiser, and T. Wangler, in *Proceedings of the Invited Papers, 14th Particle Accelerator Conference*, San Francisco, California, 1991, edited by L. Lizama and J. Chew (IEEE, New York, 1991), Vol. 1, p. 251; M. Reiser, J. Appl. Phys. **70**, 1919 (1991).

[2] R.L. Gluckstern, Phys. Rev. Lett. **73**, 1247 (1994).

[3] R. Pakter, G. Corso, T. S. Caetano, D. Dillenburg, and F. B. Rizzato, Phys. Plasmas, **12**, 4099 (1994).

[4] S. Bernal, R. A. Kishek, M. Reiser, and I. Haber, Phys. Rev. Lett. **82**, 4002 (1999).

[5] O.A. Anderson, Part. Accel. **21**, 197, (1987).

[6] S.G. Anderson and J.B. Rosenzweig, Phys. Rev. ST Accel. Beams **3**, 094201 (2000).

[7] J. M. Dawson, Phys. Rev. **113**, 383 (1959).

[8] F.B. Rizzato et al, Phys. Plasmas **14**, 110701, (2007), and references therein.

[9] H. Okamoto, Phys. Plasmas **9**, 322 (2002).

[10] F.B. Rizzato and R. Pakter, Phys. Rev. Lett. **89**, 184102, (2002).

[11] E.G. Souza, A. Endler, R. Pakter, F.B. Rizzato, R.P. Nunes, Appl. Phys. Lett. **96**, 141503 (2010).

[12] H. Okamoto and M. Ikegami, Phys. Rev. E **55**, 4694 (1997).

[13] S.M. Lund, D. P. Grote, and R. C. Davidson, Nuc. Instr. and Meth. A **544**, 472 (2005); Y. Fink, C. Chen, and W. P. Marable, Phys. Rev. E **55**, 7557 (1997); R.P. Nunes, R. Pakter, F.B. Rizzato, A. Endler, and E. G. Souza, Phys. Plasmas **16**, 033107, (2009).

[14] L. Serafini and J.B. Rosenzweig, Phys. Rev. E **55**, 7565 (1997).